Cancer Gene Therapy (2011) 18, 42–52

www.nature.com/cgt

Open

ORIGINAL ARTICLE

# Enhanced tumor therapy using vaccinia virus strain GLV-1h68 in combination with a β-galactosidase-activatable prodrug *seco*-analog of duocarmycin SA

**CM Seubert[1,5], J Stritzker[1,2,5], M Hess[1], U Donat[1], JB Sturm[1], N Chen[2], JM von Hof[3], B Krewer[3], LF Tietze[3], I Gentschev[1,2] and AA Szalay[1,2,4]**

[1]*Department of Biochemistry, Biocenter, University of Würzburg, Würzburg, Germany;* [2]*Genelux Corporation, San Diego, CA, USA;* [3]*Institut für Organische und Biomolekulare Chemie, Georg-August-Universität Göttingen, Göttingen, Germany;* [4]*Department of Radiation Oncology, Moores Cancer Center, University of California, San Diego, La Jolla, CA, USA*

Breast cancer is the most common cause of cancer-related death worldwide, thus remaining a crucial health problem among women despite advances in conventional therapy. Therefore, new alternative strategies are needed for effective diagnosis and treatment. One approach is the use of oncolytic viruses for gene-directed enzyme prodrug therapy. Here, the *lacZ*-carrying vaccinia virus (VACV) strain GLV-1h68 was used in combination with a β-galactosidase-activatable prodrug derived from a *seco*-analog of the natural antibiotic duocarmycin SA. Tumor cell infection with the VACV strain GLV-1h68 led to production of β-galactosidase, essential for the conversion of the prodrug to the toxic compound. Furthermore, drug-dependent cell kill and induction of the intrinsic apoptosis pathway in tumor cells was also observed on combination therapy using the prodrug and the GLV-1h68 strain, despite the fact that VACV strains encode antiapoptotic proteins. Moreover, GI-101A breast cancer xenografts were effectively treated by the combination therapy. In conclusion, the combination of a β-galactosidase-activatable prodrug with a tumor-specific vaccinica virus strain encoding this enzyme, induced apoptosis in cultures of the human GI-101A breast cancer cells, in which a synergistic oncolytic effect was observed. Moreover, *in vivo*, additional prodrug treatment had beneficial effects on tumor regression in GLV-1h68-treated GI-101A-xenografted mice.
*Cancer Gene Therapy* (2011) **18,** 42–52; doi:10.1038/cgt.2010.49; published online 10 September 2010

**Keywords:** vaccinia virus; breast cancer; oncolytic virotherapy; prodrug

## Introduction

Breast cancer is the most common form of cancer and the second most common cause of cancer-related death in women.[1] In the United States of America, it is estimated that 1.5 million new cases of breast cancer was diagnosed in 2009, and that ~40 400 women will die from breast cancer-related causes alone, despite advances in conventional therapy.[2] Consequently, novel, well-tolerated and more effective therapies are needed to reduce the number of breast cancer-related deaths. Among several strategies to improve currently applied treatments, the use of oncolytic viruses is a very promising therapeutic approach.[3,4]

Correspondence: Dr AA Szalay, Genelux Corporation, San Diego, CA 92109, USA.
E-mail: aaszalay@genelux.com
[5]These authors contributed equally to this work.
Received 26 July 2009; revised 10 May 2010; accepted 19 July 2010; published online 10 September 2010

Regarding the many different oncolytic viral agents used for tumor-directed therapy, vaccinia virus (VACV) has several advantages. This large DNA virus exclusively replicates in the cytoplasm without the need for host DNA-synthesis machinery, thereby excluding the risk of integration into the host genome. It displays rapid spread, a broad range of host cell tropism and a high capacity for genetic payload, with up to 25 kb of foreign DNA.[5] Moreover, the systemic injection of recombinant VACV (rVACV) strains into tumor-bearing mice resulted in high viral titers in tumors, but not in other organs, indicating tumor-specific colonization.[6–8]

Another approach is the use of viruses for gene-directed enzyme prodrug therapy (GDEPT) to improve the selectivity of chemotherapy by enabling cancer cells to convert prodrugs of low cytotoxictiy to highly potent drugs. Because the suicide genes must be expressed selectively in tumor cells to prevent adverse effects in the patient, substantial efforts have been conducted to develop gene transfer vectors specifically targeting tumors. Among these, tumor-specific viruses including adenovirus, sindbis virus, retroviruses, herpes simplex

virus, vesicular stromatitis virus and VACV so far appear to be the best-suited gene transfer vectors (reviewed in Schepelmann and Springer[9]). Using the VACV species, several promising results have already been obtained with replication-competent, cytosine deaminase-expressing VACV strains in combination with the well-described prodrug 5-fluorocytosine.[10–14] Here, a β-galactosidase-expressing VACV strain was used for GDEPT.

The β-galactosidase-encoding *lacZ* gene of *E. coli* was the first widely used reporter gene. It has numerous applications in molecular and cellular biology and has also been used as marker in clinical trials.[15,16] Moreover, a variety of substrate structures were generated to enable detection of β-galactosidase expression in live animals, by optical imaging with near-infrared fluorescent probes,[17,18] by luminescent imaging using a caged D-luciferin–galactoside conjugate,[19] with radionuclide substrates for SPECT imaging[20] and with probes enabling magnetic resonance imaging.[21] As prodrug-mediated tumor therapy has been investigated more extensively, a number of β-galactosidase-activatable prodrugs have also been described, the most promising of which are the *seco*-analogs of the highly cytotoxic natural antibiotics CC-1065 and duocarmycin SA (for a recent review see Tietze and Krewer[22]). However, no experiments have been published in the literature that describes the successful use of these prodrugs in live tumor-bearing animal studies. One of the most promising prodrugs developed so far, namely, the (1*S*)-*seco*-CBI-DMAI-β-D-galactoside 1, showed a high Q $IC_{50}$ value (Q $IC_{50} = IC_{50}$ of prodrug/$IC_{50}$ of prodrug in the presence of the cleaving enzyme, with $IC_{50}$ being the concentration required for 50% growth inhibition of target cells) of 3500 and an $IC_{50}$ value for the corresponding highly cytotoxic drug 2 of 16 pM (Supplementary Figure S1).[23] In this study, this prodrug, in combination with the β-galactosidase-encoding oncolytic VACV strain GLV-1h68, was tested in cell culture and animals, resulting in enhanced breast cancer regression.

## Materials and methods

### *Cell culture and VACV constructs*

The GI-101A human breast cancer cells were cultured in RPMI-1640 medium containing 1% HEPES (4-(2-hydroxyethyl)-1-piperazineethanesulfonic acid), 1% sodium pyruvate, 1% antibiotic–antimycotic solution and 20% fetal bovine serum (FBS). The human adenocarcinoma cells MDA-MB-231-CBG (click-beetle luciferase-expressing cells derived from MDA-MB-231; U Donat *et al*., unpublished data) were cultured in Dulbecco's modified Eagle's medium, 10% FBS and 10 μg ml$^{-1}$ blasticidin. Canine breast adenoma ZMTH3 cells were cultured in RPMI-1640 medium containing 20% FBS.

GLV-1h68 was derived from VACV LIVP as described previously.[7] In GLV-1h43, the *lacZ*-containing gene cassette was replaced by a nonrelevant gene-containing cassette. Both strains were developed from the VACV LIVP strain by site-directed insertional mutagenesis. The *F14.5L* locus was replaced by insertion of a *Renilla* luciferase–*GFP* (green fluorescent protein) fusion construct under the control of a synthetic early/late promoter ($P_{SEL}$). The hemagglutinin (*HA*) gene was replaced by the β-glucuronidase-encoding gene *gusA* and placed under the control of the late promoter P11. The viral thymidine kinase (*TK*) was either replaced by *lacZ*, the gene encoding β-galactosidase, controlled by the VACV early/late P7.5 promoter in GLV-1h68, or by a nonrelevant gene construct in GLV-1h43 (Figure 1a). The virus strains GLV-1h71 and

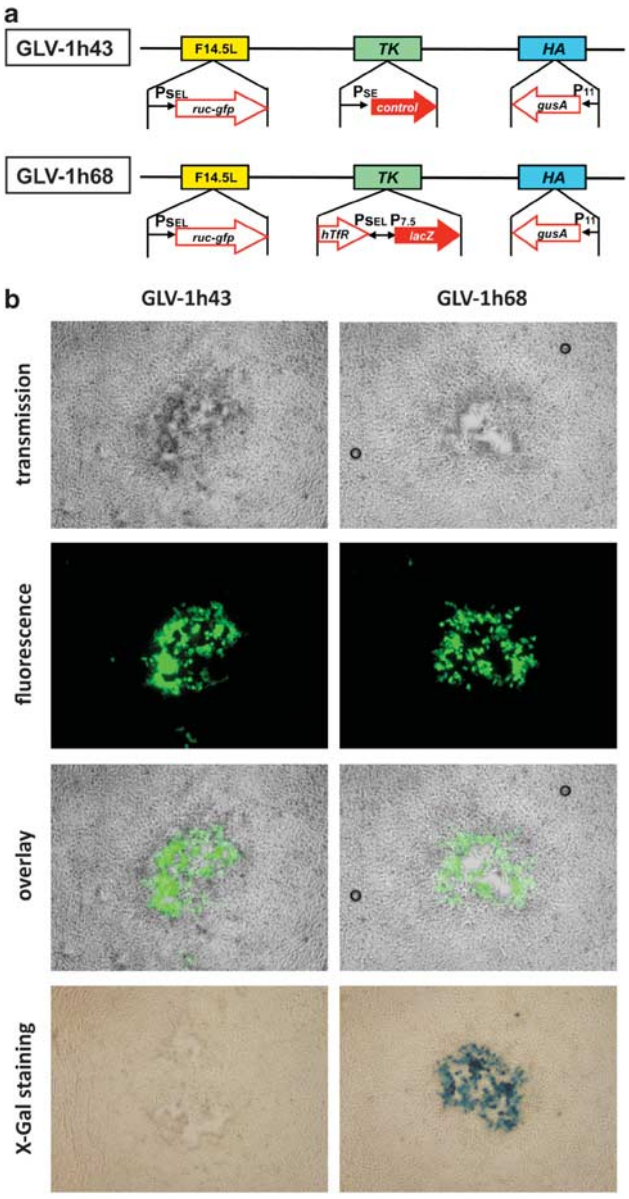


**Figure 1** Recombinant vaccinia virus (rVACV) constructs and marker gene expression. (**a**) The wild-type LIVP was used for the generation of modified rVACV with designations of GLV-1h43 and GLV-1h68. *P11*, VACV late P11 promoter; *PE/L*, VACV synthetic early/late promoter; *P7.5*, VACV 7.5 K early/late promoter. (**b**) Expression of the marker gene green fluorescent protein (GFP) could be detected in plaques of both virus strains, whereas staining for X-gal revealed expression of β-galactosidase in GLV-1h68-infected GI-101A cells only. HA, hemagglutinin; TK, thymidine kinase.

GLV-1h85 are the *Ruc-GFP*-negative analogs of GLV-1h68 and GLV-1h43, respectively.

### *Infections of cell cultures*

At 2 days before infection, cells were seeded in six-well plates for RNA and protein isolation, and in 24-well plates for survival and microscopy studies. If not otherwise indicated, the 90% confluent cell layer was mock infected or infected with GLV-1h43 or GLV-1h68 at a multiplicity of infection per cell of 0.05 or 0.5 for 1 h at 37 °C in medium containing 2% FBS. The virus-containing medium was then aspirated and replaced by non-prodrug-containing cell culture medium or medium supplemented with 10 nM of prodrug.

### *Isolation and detection of proteins*

At 6, 12, 24, 48 or 72 h post-infection (hpi), cells were harvested and lysed in SDS sample buffer or in lysis buffer (10 mM Tris (pH 7.4), 150 mM NaCl, 1 mM EDTA, 10 mM HEPES, 0.05% Igepal and 0.75 mM dithiothreitol) supplemented with a proteinase inhibitor cocktail (Roche, Penzberg, Germany). The cell lysates were separated on a 10, 12 or 15% SDS-polyacrylamide electrophoresis gel, and proteins were transferred onto a nitrocellulose transfer membrane (Whatman GmbH, Dassel, Germany). The membrane was then incubated with one of the following: anti-β-actin mouse monoclonal antibody (ab6276, Abcam, Cambridge, UK), anti-β-galactosidase rabbit polyclonal antibody (A-11132, Molecular Probes, Leiden, the Netherlands), anti-cleaved caspase-3 rabbit polyclonal antibody (no. 9661, Cell Signaling Technology, Danvers, MA), anti-full-length caspase-3 rabbit polyclonal antibody, (no. 9662, Cell Signaling Technology), anti-caspase-8 mouse monoclonal antibody (no. 9746, Cell Signaling Technology), anti-caspase-9 rabbit polyclonal antibody (no. 9502, Cell Signaling Technology), anti-GFP rabbit polyclonal (sc-8334, Santa Cruz, Heidelberg, Germany) or anti-cleaved poly (ADP-ribose) polymerase (PARP) mouse monoclonal antibody (51-9000017, BD Pharmingen, Heidelberg, Germany). The first antibodies were then detected using horseradish peroxidase-labeled anti-mouse (ab6728, Abcam) or anti-rabbit (ab6721, Abcam) secondary antibodies, followed by enhanced chemiluminescence.

Quantitative results were obtained using a NightOWL LB 981 imaging system (Berthold Technologies, Bad Wildbad, Germany).

### *Analysis of RNA expression*

At 6, 12, 24, 48 or 72 hpi, cellular RNA was isolated using the RNeasy Mini Kit (Qiagen, Hilden, Germany), followed by DNase treatment using DNA-free Kit (Ambion, Austin, TX). RNA samples were converted to cDNA by RevertAid First Strand cDNA Synthesis Kit (Fermentas, St Leon-Rot, Germany) and analyzed by reverse transcriptase PCR and quantitative PCR using primers for glyceraldehyde 3-phosphate dehydrogenase (from First Strand cDNA Synthesis Kit (Fermentas)); for β-actin, the primers used were forward: 5′-GGAGAA AATCTGGCACCACAC-3′ and reverse: 5′-CCATCTCT TGCTCGAAGTCCA-3′; for *lacZ*, forward: 5′-GGC CAGTTGCGTGACTACC-3′ and reverse: 5′-CCGACA TCGCAGGCTTCTG-3′ for real-time PCR and 5′-CAC GGCATTAAAGTTGTTCTGCTTC-3′ for reverse transcriptase PCR; and for GFP, forward: 5′-GCGTG CAGTGCTTTTCCAG-3′ and reverse: 5′-AGGGCAGA CTGGGTGGAC-3′.

Quantitative PCR was performed using ABsolute QPR SYBR Green Mix (Thermo Scientific, Epsom, UK) in a DNA Engine Opticon CFD-0200 (MJ Research, Waltham, MA) and analyzed using the Opticon Monitor software (MJ Research).

### *β-Galactosidase assays and X-gal staining*

The concentration of cell-associated β-galactosidase, as well as the concentration in the supernatant, was analyzed in a β-galactosidase assay. A standard dilution series was performed over the range of $1 \times 10^{-6}$–1 U $\mu l^{-1}$ β-galactosidase (from *Aspergillus oryzae*—11.2 U $mg^{-1}$, G5160, Sigma-Aldrich, Steinheim, Germany). Tumor homogenates, blood serum samples, cell lysates and cell culture supernatants were incubated with the staining solution (40 µl X-gal in dimethylformamide (40 mg $ml^{-1}$), ferricyanide (12 mM K3Fe(CN)6), 5.2 mM MgCl2 and ferrocyanide solution (12 mM K4Fe(CN)6)), and optical density was determined in a Tecan sunrise absorbance reader (Tecan, Crailsheim, Germany).

For X-gal staining, cells on coverslips or tumor sections were incubated with the staining solution overnight at room temperature, washed several times with PBS and mounted in 80% glycerol in PBS.

### *Histology and fluorescent microscopy*

For the microscopical analysis of β-galactosidase and GFP expression, GI-101A cells were seeded on coverslips and infected using 100 plaque-forming units (PFUs) per well. After 2 days, cells were fixed for 2 min using 4% paraformaldehyde and washed in PBS. Subsequently, either direct visualization was performed for GFP or β-galactosidase staining was carried out before microscopical analysis by means of a Leica DMR fluorescence microscope (Leica, Wetzlar, Germany) and a Diagnostic Instruments digital camera model 2.3.1 (Visitron Systems GmbH, Puchheim, Germany) using Meta-Vue 5.0r2 software (Visitron Systems GmbH).

Histology and fluorescence microscopy of tumor sections were performed as described previously.[24] Briefly, snap-frozen GI-101A tumors of GLV-1h43- or GLV-1h68-injected mice were fixed in 4% paraformaldehyde and 100 µm vibratome tissue sections were permeabilized in PBS containing 0.3% Triton X-100. Neighboring sections were then stained using X-gal and Hoechst 33342. After several rinses in PBS, tissue sections were incubated in PBS containing 60% (v/v) glycerol and then mounted in PBS containing 80% (v/v) glycerol.

Tumor specimens were examined with the Stereo-Fluorescence microscope (MZ16 FA, Leica, Heerbrugg, Switzerland) equipped with a digital CCD camera (DC500, Leica). The blue β-galactosidase staining was visualized using white light, whereas GFP and Hoechst

33342 were detected using fluorescence. Digital images ($1300 \times 1030$ pixel color images) were processed with Photoshop 10.0 (Adobe Systems, San Jose, CA) and merged to yield pseudocolored pictures.

### *Prodrug synthesis*

Prodrug synthesis was performed as described previously[23] and stock solutions of the prodrug were prepared in dimethyl sulfoxide.

### *Cell viability assay*

The amount of viable cells after infection with GLV-1h43 or GLV-1h68 and/or treatment with 10 nM prodrug was measured using 3-(4,5-dimethylthiazol-2-yl)-2,5-diphenyltetrazolium bromide (MTT) (Sigma, Taufkirchen, Germany). At the indicated time points, the medium was replaced by 0.5 ml MTT solution at a concentration of 2.5 mg $ml^{-1}$ MTT dissolved in RPMI 1640 medium without phenol red and incubated for 4 h at 37 °C in a 5% $CO_2$ atmosphere. After removal of the MTT solution, 1 N HCl diluted in 2-propanol was added and the optical density was then measured at a wavelength of 570 nm. Mock-infected cells served as a reference and were considered as 100% viable.

The rate of apoptosis was determined using the PE-annexin V apoptosis detection kit (BD Biosciences, Heidelberg, Germany) according to the manufacturer's instructions. The analysis was performed on a Epics XL flow cytometer (Beckman Coulter GmbH, Krefeld, Germany) and the data were analyzed using WinMDI 2.8 (Joe Trotter, Scripps Research Institute, La Jolla, CA).

### *Animal studies*

GI-101A xenograft tumors were developed in 6- to 8-week-old female nude mice (NCI:Hsd:Athymic Nude-*Foxn1*$^{nu}$, Harlan, Borchem, Germany and Indianapolis, IN) by implanting $5 \times 10^6$ GI-101A cells subcutaneously on both hind flanks (two tumors per mouse). Tumor growth was recorded once a week in two dimensions using a digital caliper. Tumor volume was calculated as $((\text{length} \times \text{width}^2)/2)$ and reported in $mm^3$. At 30 days after tumor cell implantation, three groups of 12 mice were injected with a single intravenous dose of PBS, or $5 \times 10^6$ PFUs of GLV-1h43 or GLV-1h68 in 100 µl of PBS. The 12 mice of each group were subdivided into two groups of six mice that were intraperitoneally injected three times a week with 200 µl of a 1:1 (v/v) mixture of dimethyl sulfoxide and PBS alone or 200 µl of the same mixture containing prodrug (100 nM), starting 6 days after VACV injection.

All animal experiments were carried out in accordance with protocols approved by the Institutional Animal Care and Use Committee of Explora Biolabs (San Diego, CA) or the 'Regierung von Unterfranken' (Würzburg, Germany).

### *Statistical analysis*

The significance of differences between the various groups was determined using a two-tailed unpaired *t*-test (Excel 2008 for Mac, Microsoft, Redmond, WA). A *P*-value $<0.05$ was considered significant.

## Results

### *β-Galactosidase-activatable prodrug: mechanism of action*

The recently described *seco*-duocarmycin SA analog-derived prodrug 1 (Supplementary Figure S1) used in this study was previously shown to be extremely efficient in killing cells in culture.[23] On β-galactosidase activation, prodrug 1 releases a drug with an $IC_{50}$ value of 16 pM that is 3500 times more cytotoxic than the prodrug itself. However, studies have not yet determined whether target cell death also occurred via the same intrinsic apoptosis mechanism as already described for duocarmycin SA.[25–27]

We therefore incubated GI-101A cells with PBS and prodrug alone or prodrug in combination with purified β-galactosidase. In contrast to PBS or prodrug-only treated cells, Hoechst 33342 staining showed nuclear condensation in a high proportion of prodrug and β-galactosidase-treated cells. A parallel staining with propidium iodide, which is only permeant into dead cells, was mostly negative. This indicated an intact cell membrane and supported the notion of apoptosis induction (data not shown).

To validate that the apoptosis was induced, cellular proteins were harvested and analyzed by western blotting using antibodies against cleaved PARP, caspase-3, caspase-8 and caspase-9 (Figure 2). It was obvious that cleaved PARP and cleaved caspase-3, as indicators for apoptosis,[28] were only detectable in cells that were treated with the prodrug in combination with β-galactosidase, but absent in PBS and prodrug-only controls. Furthermore,

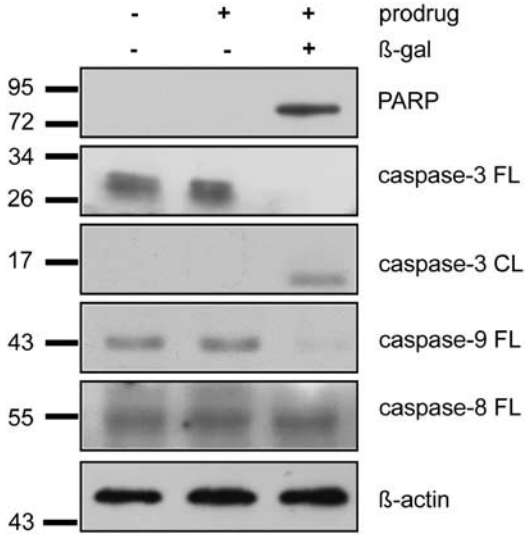


**Figure 2** Validation of apoptosis induction on prodrug activation. Western blot analysis with antibodies against cleaved poly (ADP-ribose) polymerase (PARP), full-length (FL) caspase-3, cleaved (CL) caspase-3, full-length caspase-9, full-length caspase-8 and β-actin. Cleaved PARP and cleaved caspase-3, as indicators for apoptosis, were only detectable in both prodrug and β-galactosidase-treated cells. Additionally, full-length caspase-9 concentration significantly decreased because of treatment with prodrug and β-galactosidase, whereas caspase-8 remained uncleaved. Equal protein loading was confirmed by detection of β-actin.

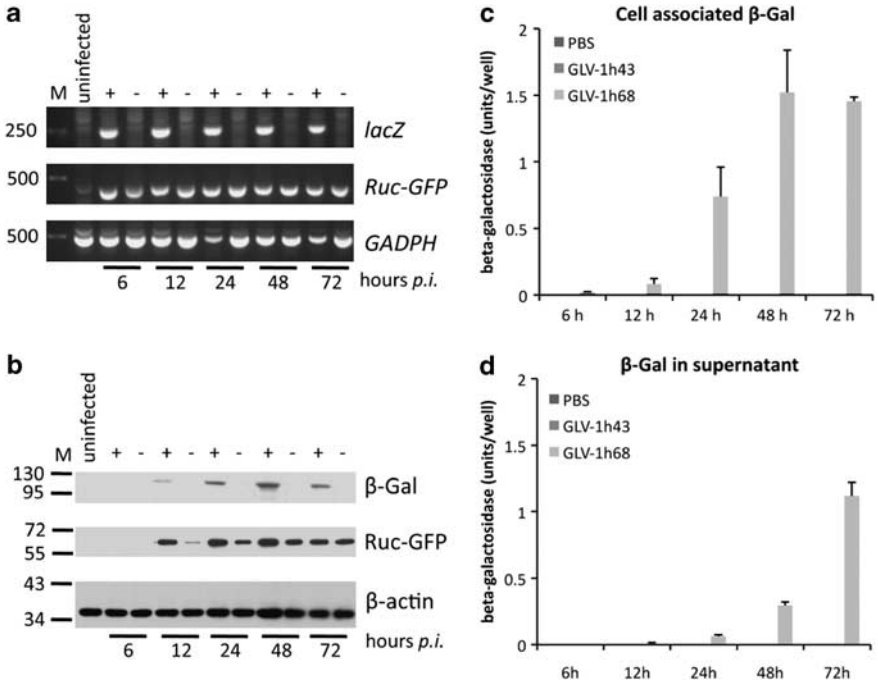


**Figure 3** Evaluation of reporter gene expression after infection with recombinant vaccinia virus (rVACV). (**a**) Reverse transcriptase PCR results from mock-infected cells (untreated), GLV-1h68- (68) or GLV-1h43 (43)-infected cells at 6, 12, 24, 48 and 72 hpi using *lacZ*-, green fluorescent protein (GFP)- and glyceraldehyde 3-phosphate dehydrogenase-specific primers. Infection with GLV-1h68 led to production of *Ruc-GFP* and *lacZ*-specific transcripts as early as 6 hpi, whereas in GLV-1h43-infected cells, no *lacZ* transcript could be detected. Both reporter gene transcripts were not detectable in mock-infected cells. (**b**) Western blot analysis using β-galactosidase (β-gal) and Ruc-GFP-specific antibodies, showing no expression of β-galactosidase in GLV-1h43-infected cells. In contrast, both proteins could be detected in GLV-h168-infected cells after 12 hpi. β-galactosidase expression increased up to 48 hpi. Equal protein loading was confirmed by detection of β-actin. (**c**, **d**) Determination of β-galactosidase activity in cell lysates (**c**) and supernatants (**d**) after infection with GLV-1h43, GLV-1h68 and mock infection. Enzyme activity in cell lysates increased up to 48 hpi with GLV-1h68, further supporting the western blot results. In supernatants, no active enzyme could be detected until 12 hpi, but then increased until 72 hpi. As expected, no active enzyme could be detected in mock- or GLV-1h43-infected cells or supernatants at all time periods. PBS, phosphate-buffered saline.

although caspase-8 remained uncleaved, the amount of full-length caspase-9 dropped significantly in prodrug and β-galactosidase-treated cells, indicating that apoptosis is induced via the intrinsic rather than extrinsic pathway.[29,30]

### *Characterization of rVACV strains GLV-1h68 and GLV-1h43 in cell culture*

To test the expression of the reporter proteins Ruc-GFP and β-galactosidase, the human breast cancer cell line GI-101A was infected with the rVACV strains GLV-1h68 or GLV-1h43 (Figure 1a). As previously mentioned, β-galactosidase was used as a prodrug-activating protein in this study.

As expected, expression of GFP could be observed for both strains by fluorescence microscopy, whereas β-galactosidase-specific X-gal staining of plaques was only positive in GLV-1h68-infected GI-101A cells (Figure 1b).

Reverse transcriptase PCR analysis (Figure 3a) and western blotting (Figure 3b) confirmed the virus-mediated expression of the reporter genes. No *Ruc-GFP*- or *lacZ*-specific transcripts or proteins could be detected in mock-infected control cells, whereas both were detectable in GLV-1h68-infected cells. In contrast, infection with GLV-1h43 led to production of Ruc-GFP but not β-galactosidase. Although reporter gene transcripts could be detected as early as 6 hpi, the respective proteins were not detected by western blot until 12 hpi. In addition, real-time PCR revealed an increasing *lacZ* expression until 48 hpi (data not shown), correlating with the western blot analysis (Figure 3b) of GLV-1h68-infected cells.

As the prodrug is converted only by a functional enzyme, we also determined the β-galactosidase activity in cell lysates (Figure 3c) and supernatants (Figure 3d) of mock-, GLV-1h43- and GLV-1h68-infected GI-101A cells. The enzyme activity increased until 48 hpi in the cell lysates, as supported by the western blot results (Figure 3b). In supernatants, no β-galactosidase activity was detected by 12 hpi, but then increased by 72 hpi, probably as a consequence of increased viral cell lysis. In mock- or GLV-1h43-infected cells, no β-galactosidase activity was detectable at any time points.

Furthermore, when coincubating the cell lysates and supernatants of mock-, GLV-1h43- or GLV-1h68-infected cells with uninfected GI-101A cells, the observed prodrug-mediated cell death correlated with the presence of active β-galactosidase (Supplementary Figure S2).

Therefore, a β-galactosidase-specific prodrug should only be activated on GLV-1h68 infection.

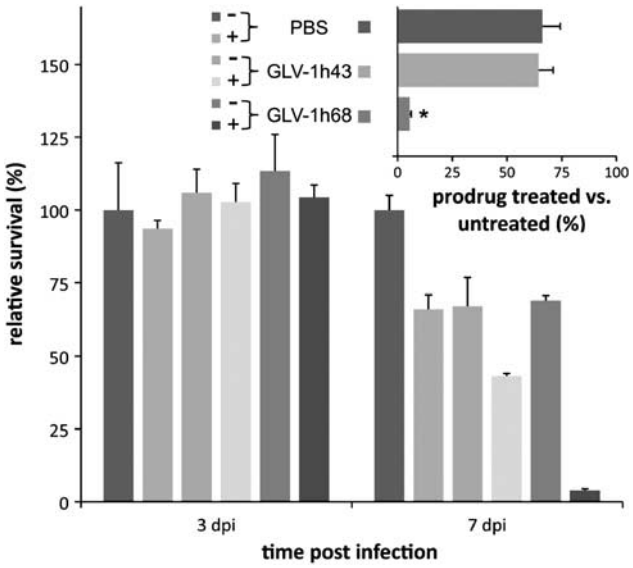


**Figure 4** Cell survival studies after prodrug treatment and infection. Cells were infected with a low multiplicity of infection of 0.05 or mock infected and treated with 10 nM prodrug. Non-prodrug-treated cells served as the control. Cell viability was determined by 3-(4,5-dimethylthiazol-2-yl)-2,5-diphenyltetrazolium bromide (MTT)-assays on days 3 and 7 post-infection. On day 3 post-infection, no significant difference in cell viability between the different samples was observed. Combined treatment of cells with GLV-1h68 and prodrug induced a significantly higher tumor cell kill 7 days post-infection compared with infection with GLV-1h68 alone. Although prodrug treatment alone as well as rVACV treatment alone had inhibitory effects when compared with untreated cells (significance not shown), only simultaneous treatment of cells with GLV-1h68 and prodrug contributed to strong synergistic effects and the most efficient cell killing (inset, showing survival of prodrug-treated vs corresponding untreated cells). In each chart, average plus standard deviation ($n=3$) is shown. Asterisk indicates statistical significance ($P<0.05$). PBS, phosphate-buffered saline.

### *Enhanced tumor cell lysis after GLV-1h68 infection due to prodrug addition*

In tumors treated with oncolytic VACV, not every cell is infected and will express β-galactosidase; hence, sufficient prodrug bystander effects are needed for enhancement of oncolysis.[11]

We therefore chose to use a low multiplicity of infection of 0.05 for experiments, applying the prodrug directly in combination with mock-, GLV-1h43- and GLV-1h68-infected cells. The prodrug was added at a concentration of 10 nM immediately after infection. Non-prodrug-treated cells served as controls. Cell survival was analyzed by MTT assays on days 3 and 7 after infection.

As shown in Figure 4, on day 3 post-infection, no significant difference was observed between prodrug-treated or untreated mock-, GLV-1h43- or GLV-1h68-infected cells. Conversely, simultaneous treatment of GI-101A cells with GLV-1h68 and 10 nM of prodrug resulted in significantly higher tumor cell killing at 7 days post-infection compared with GLV-1h68 alone. The prodrug alone had some inhibitory effects on mock- or GLV-1h43-infected GI-101A cells, resulting in an ~30% reduction of cell numbers on day 7 post-infection, when compared with the respective non-prodrug-treated controls. However, only the combination of the prodrug with GLV-1h68 resulted in strong synergistic effects and the most efficient cell killing (Figure 4, inset).

Similar effects were also observed when using other breast tumor cells such as the human breast adenocarcinoma cells MDA-MB-231-CBG and canine breast adenoma ZMTH3 (data not shown).

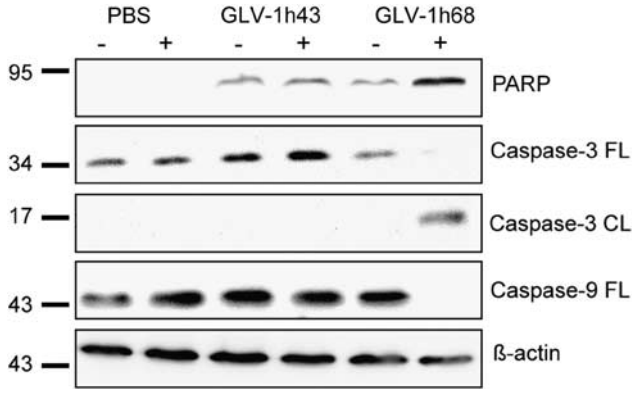


**Figure 5** Apoptosis induction in GLV-1h68-infected tumor cells on prodrug treatment. Western blot analysis using specific antibodies against cleaved poly (ADP-ribose) polymerase (PARP), full-length (FL) caspase-3, cleaved (CL) caspase-3, full-length caspase-9 and β-actin. Samples were taken from infected or mock-infected GI-101A cells treated (+) or untreated (−) with 10 nM prodrug. Expression of the apoptosis indicator PARP was significantly higher in GLV-1h68-infected cells treated with prodrug, compared with cells treated with vaccinia virus alone or with GLV-1h43 and prodrug. Uninfected control cells showed almost no expression of PARP. Furthermore, approximately no full-length caspase-3 or caspase-9 could be observed in GLV-1h68-infected cells treated with prodrug, whereas both proteins were present in the other samples. Cleaved caspase-3 was detectable only in those samples retrieved after combined treatment with GLV-1h68 and prodrug. Equal loading of protein was confirmed by detection of β-actin. PBS, phosphate-buffered saline.

### *Induction of apoptosis in GLV-1h68-infected tumor cells after addition of prodrug*

VACV encodes a number of antiapoptotic factors and inhibits both the extrinsic as well as the intrinsic apoptotic pathway (reviewed in Taylor and Barry[31]). To test whether these factors can also prevent cells from (pro)drug-mediated apoptosis, we analyzed the induction of apoptosis by measuring the binding of labeled annexin V using flow cytometry. As both GLV-1h68 and GLV-1h43 result in very high expression levels of the fusion protein Ruc-GFP, which interfered with the flow cytometry measurements, we used two other VACV strains, namely GLV-1h71 (β-galactosidase-positive) and GLV-1h85 (β-galactosidase-negative), which do not express the fluorescent protein. At 3 days post-infection, we detected $59.9 \pm 1.1\%$ annexin V-positive cells in prodrug-treated cells infected with GLV-1h71, but only $39.9 \pm 4.4\%$ cells when GLV-1h85 was used. This corresponded well with $40.2 \pm 1.9\%$ apoptotic cells in GLV-1h71-infected cells that were not treated with

prodrug. Therefore, the enhanced rate in apoptosis could be attributed to the prodrug treatment.

Even clearer results were obtained when analyzing protein lysates of prodrug-treated or untreated mock-, GLV-1h43- and GLV-1h68-infected cells, using western blotting with antibodies against cleaved PARP, caspase-3 and caspase-9 (Figure 5).

The quantitative analysis of the western blots revealed a sevenfold higher concentration of cleaved PARP in cells treated with GLV-1h68 in combination with the prodrug, when compared with cells treated with VACV alone or with GLV-1h43 and the prodrug. In GI-101A cells not infected with rVACV, almost no cleaved PARP was detectable. Even more pronounced was the difference with cleaved caspase-3, which could only be detected in GLV-1h68-infected cells treated with prodrug. On the other hand, an at least threefold less full-length caspase-3 and a sevenfold less full-length caspase-9 was present in GI-101A cells treated with prodrug after infection with GLV-1h68 compared with controls. The induction of apoptosis, therefore, can still be observed in the presence of VACV and is specifically induced in cells treated with prodrug and the β-galactosidase-encoding GLV-1h68 strain.

### *Enhanced GLV-1h68-mediated oncolysis on prodrug treatment*

Next, we investigated the oncolytic potential of a combined treatment using the β-galactosidase-activatable prodrug and the rVACV strain GLV-1h68 in the GI-101A xenograft breast cancer model.

As active β-galactosidase might be released from GLV-1h68-infected tumors into the blood stream and lead to unwanted side effects in other tissues, the β-galactosidase activity in tumors and in blood serum samples was tested in a preliminary experiment. Three GI-101A tumor-bearing mice were injected with GLV-1h68, and at 42 days post-infection, the mice were killed. Tumor homogenates and blood serum samples were then analyzed by β-galactosidase assay. The results revealed high enzyme activity in tumor samples ($\sim 100\,U\,g^{-1}$ tumor tissue), but undetectable levels in blood serum samples (detection limit: $0.3\,U\,ml^{-1}$). Therefore, unwanted side effects are unlikely to occur. Thus, we began to determine the effects of the β-galactosidase-activatable prodrug in combination with the *lacZ*-encoding GLV-1h68 strain in live animals.

For this purpose, mice were subcutaneously injected with $5 \times 10^6$ GI-101A cells on each flank, which formed tumors of around $450\,mm^3$ after 30 days. Groups of 12 mice were then intravenously injected with PBS or with $5 \times 10^6$ PFUs each of both GLV-1h43 and GLV-1h68 cells. The animals were then subdivided equally into two groups. At 6 days after rVACV injection, prodrug treatment was started in one subgroup, whereas the other subgroup received injections of a 1:1 (v/v) mixture of dimethyl sulfoxide and PBS only (Figure 6).

Tumor size measurements revealed that both rVACV strains showed tumor therapeutic efficacy compared with PBS-injected mice, with the PBS-injected mice having to be killed because of tumor burden between 6 and 9 weeks post-injection. Interestingly, GLV-1h43-mediated tumor therapy was more effective compared with GLV-1h68 treatment. The injection of the prodrug resulted in reduced tumor size in all subgroups when compared with the corresponding non-prodrug-treated animals, although the difference did not reach statistical significance in those groups injected with PBS or the GLV-1h43 strain ($P > 0.15$). In contrast, the subgroup treated with prodrug after injection of the *lacZ*-encoding GLV-1h68 strain had a significantly decreased tumor volume ($P < 0.006$) at 70 days after rVACV injection, when compared with the non-prodrug-treated GLV-1h68-injected control. The tumor size in the prodrug-treated subgroup was reduced close to the initial tumor volume before injection of VACV, whereas the non-prodrug-treated subgroup had an average tumor volume of $\sim 930\,mm^3$.

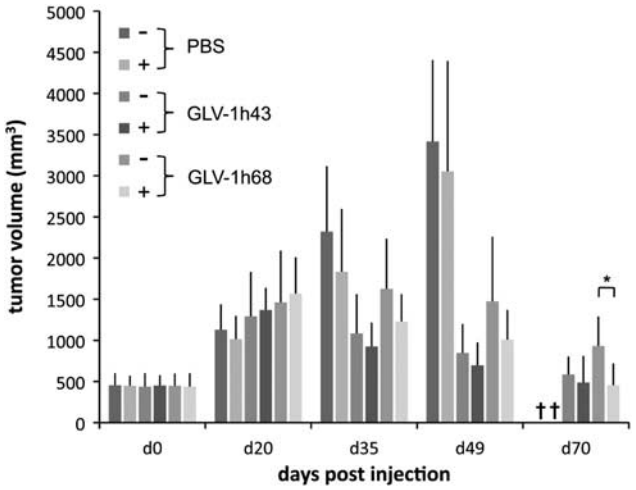


**Figure 6** Characterization of tumor progression and oncolysis on recombinant vaccinia virus (rVACV) and prodrug treatment. Groups of 12 GI-101A tumor-bearing mice (two tumors on each) were injected intravenously with phosphate-buffered saline (PBS), or $5 \times 10^6$ PFUs of GLV-1h43 and GLV-1h68. Although one subgroup of six mice received prodrug treatment, the other subgroup received injections of 50% dimethyl sulfoxide/50% PBS only. Tumor size was measured weekly until 70 dpi for rVACV-infected mice or until the mice had to be killed because of tumor burden in PBS-injected control groups. Injection of prodrug led to reduced tumor size in all subgroups compared with untreated mice, but reached no statistical significance except in the GLV-1h68-treated group on day 70 after rVACV injection. Depicted are average values plus standard deviation. Asterisk indicates statistical significance ($P < 0.05$) between prodrug-treated and untreated subgroups.

### *Prodrug treatment: effects on viral tumor colonization*

As prodrug conversion and cell killing might lead to inhibition of viral replication or enrichment of *lacZ*-negative mutants of GLV-1h68 within the tumor, both prodrug-treated and untreated tumors of mice were isolated 71 days after rVACV injection, and the amount of virus was determined by standard plaque assay (Supplementary Figure S3a). No significant differences ($P > 0.42$) were observed between prodrug-treated or untreated GLV-1h43- and GLV-1h68-injected mice.

Furthermore, sterile-filtered (0.1 μm) tumor lysates were used to activate prodrug in cell culture experiments (Supplementary Figure S3b). For this purpose, lysates of two tumors per subgroup were diluted in cell culture medium (resulting in lysate of 20 mg tumor tissue in 1 ml cell culture medium). This was then added to GI-101A cells and MTT assays were performed 2 days later. Added prodrug was converted and resulted in cell killing when tumor lysates were derived from mice injected with GLV-1h68, regardless of previous prodrug treatments in the living animals. On the other hand, no killing was observed in non-prodrug-treated GI-101A cells or in cells that were treated with tumor lysates derived from GLV-1h43-injected mice.

In addition, adjacent tumor sections of prodrug-treated GLV-1h43- or GLV-1h68-injected mice were analyzed for the presence of GFP and β-galactosidase activity (Supplementary Figure S3c). Both viral constructs led to large patches of GFP within the tumor tissue, which was depicted using Hoechst 33342 staining. Using X-gal staining, functional β-galactosidase was detected in GLV-1h68-infected tumors only and correlated with the GFP-positive regions. Furthermore, plaques obtained from prodrug-treated GLV-1h68-injected mice and analyzed by X-gal staining revealed that all plaques stained positive for β-galactosidase. Therefore, prodrug treatment did not lead to a selection of GLV-1h68 mutants with nonfunctional β-galactosidase or to a reduction of VACV titers in tumors.

Taken together, our data showed that a combination of the oncolytic, *lacZ*-encoding VACV strain GLV-1h68 with a β-galactosidase-activatable prodrug could induce apoptosis in breast cancer cells and led to accelerated tumor shrinkage in a xenograft mouse model.

## Discussion

In this work, the mode of action and the effects of a combination therapy using an oncolytic VACV strain, together with a β-galactosidase-activatable prodrug on tumor regression, were analyzed in a breast cancer xenograft mouse model system. The used human breast cancer cell line GI-101A was derived from cells isolated from a 57-year-old female cancer patient with recurrent, infiltrating ductal adenocarcinoma.[32,33] It has been previously shown that xenograft tumors derived from GI-101A cells are eradicated on treatment with GLV-1h68,[7] the onolytic VACV strain also used in this study.

Cell culture experiments revealed that GLV-1h68 as well as the control virus strain GLV-1h43 lacking the *lacZ* gene insert, both infected and replicated equally well within GI-101A cells (Figure 1 and data not shown). Because only functionally active enzyme leads to conversion of the prodrug, it was important to analyze the increasing β-galactosidase activity in cell lysates and supernatants of GLV-1h68-infected GI-101A cells (Figures 3b–d). Activation of the prodrug was achieved by coincubation with the sterile-filtered, β-galactosidase-containing cell lysates and supernatants, resulting in killing of GI-101A cells (Supplementary Figure S2). Conversely, incubation with samples obtained from mock- or GLV-1h43-infected cells did not change overall survival. Furthermore, the prodrug-mediated killing observed in the presence of sterile-filtered samples proved that the active drug does penetrate cell membranes, suggesting that each cell in the tumor tissue may not necessarily have to express β-galactosidase to become eliminated by the GDEPT.

Strong synergistic effects could also be observed in the combined prodrug and the GLV-1h68 strain treatment using a low multiplicity of infection of 0.05 in GI-101A cells. The prodrug itself also resulted in significant cell inhibition at 7 days post-application when compared with non-prodrug-treated mock- or GLV-1h43-infected cells. Presumably, cell growth was inhibited by the cytotoxicity of the prodrug itself, which is comparable with that of the cytotoxicity of doxorubicin.[23] However, this unspecific cell growth inhibition was much lower when compared with the additive effects observed on prodrug treatment in combination with GLV-1h68 infection. Similar results were also obtained in other human or canine breast cancer cell lines (data not shown). Canine breast cancer cells were also shown to be infected and lysed with GLV-1h68 alone.[34] The use of several breast cancer cell lines, therefore, provided evidence for a broader application spectrum of the combined prodrug rVACV approach. In addition, we also performed low-light imaging with click-beetle luciferase-expressing GI-101A-CBG and MDA-MB-231-CBG cells (data not shown), which supported the results obtained by MTT assays. Taken together, the prodrug has been cleaved on GLV-1h68-mediated expression of β-galactosidase and, thus, resulted in the release of the cytotoxic drug 2 as a *seco*-analog of the antibiotic duocarmycin SA, which was found to penetrate cell membranes and therefore caused bystander effects in breast cancer cells in culture.

It was reported that duocarmycin SA causes sequence-selective alkylation of N3 of adenine in AT-rich sites of the minor groove of DNA and induces apoptosis.[27,35] The DNA damage results in cleavage of full-length caspase-9, subsequent activation of caspase-3 and, ultimately, cell death.[25,26] As shown in Figure 2, apoptosis induction via the intrinsic pathway was confirmed by the detection of cleaved PARP, cleaved caspase-3 and the full-length caspase-8, as well as the decrease of full-length caspase-3 and -9, in cells treated with a mixture of prodrug and purified β-galactosidase.

Notably, it was reported that poxviruses, such as VACV, possess a number of mechanisms counteracting apoptosis (reviewed in Taylor and Barry[31]). Specifically, VACV-infected cells seem to be protected from the intrinsic apoptotic pathway involving cytochrome *c* release and cleavage of caspase-9.[36–40]

We therefore analyzed whether the apoptotic cascade, observed after prodrug treatment in the presence of purified β-galactosidase, was still activated in GLV-1h68-infected cells. Indeed, we were able to detect high amounts of cleaved PARP in GI-101A cells treated with prodrug

and the β-galactosidase-expressing rVACV strain. We found that lower amounts of cleaved PARP were present in controls infected with GLV-1h68 alone or with GLV-1h43 in the presence or absence of prodrug, whereas almost no cleaved PARP could be detected in mock-infected cells. Consequently, rVACV infection probably led to activation of the apoptotic pathway in some of the infected GI-101A cells, but was much higher in GLV-1h68-infected and prodrug-treated cells. The difference was even more pronounced when looking at cleaved caspase-3, which could only be detected in prodrug-treated cells expressing β-galactosidase. In conclusion, apoptosis was not inhibited by the infecting rVACV and caspase-9 cleavage confirmed the activation of the intrinsic pathway.

As we could not formally exclude that only noninfected cells underwent apoptosis because of the observed bystander effect, prodrug-treated GI-101A cells infected with the GLV-1h68 strain were stained with Hoechst 33342 and propidium iodide. Subsequent fluorescence microscopy revealed condensed nuclei also in GFP-containing, PI-negative cells (data not shown), and therefore supported the assumption that the activated prodrug can overcome the rVACV-mediated antiapoptotic mechanisms, at least in some cells. On the other hand, cells infected with rVACV and not undergoing apoptosis were also detected. Such cells will die of the VACV infection and enhance viral shedding, which will contribute to ongoing β-galactosidase production.

A similar mechanism could also explain that the titer of VACV was not decreased significantly on prodrug treatment in tumors of live animals (Supplementary Figure S3a). Another explanation for this observation could be the enrichment of mutants in *lacZ*. This, however, could be excluded as prodrug-treated, GLV-1h68-infected tumors still stained positive using X-gal (Supplementary Figure S3c). Consistently, X-gal staining was used to confirm functional β-galactosidase expression in plaques resulting from VACV titer analysis of prodrug-treated tumors from GLV-1h68-injected mice (data not shown). Finally, the applied prodrug, in contrast to the released active drug, is not able to penetrate cell membranes.[23] Therefore, the activation of the prodrug occurs in the extracellular matrix of the tumor after release of β-galactosidase from VACV-infected (lysed) cells and does not have direct influence on the infection process itself. As reported earlier and illustrated in Figure 3, the β-galactosidase is reasonably stable and remains active after cell lysis. This is also supported by microscopic analysis of tumor sections in which X-gal staining was positive in regions of GFP fluorescence, which were also characterized by low levels of actin staining and therefore lower levels of living cells (data not shown). Furthermore, we showed that the highest proportion of the enzyme remains in the tumor or is inactivated or excreted after obtaining access to the blood circulation. Otherwise, the cleavage of the prodrug had resulted in systemic toxicity. As no sign of malaise or weight loss was observed in prodrug-treated mice when compared with the respective control mice (data not shown), we concluded that the active β-galactosidase released from the tumor was negligible.

Taken together, the injected GLV-1h68 strain could replicate in tumors of live mice, regardless of prodrug therapy and did not lose its necessary ability to express functional β-galactosidase. Even more importantly, prodrug treatment of GLV-1h68-injected mice resulted in effects leading to additional tumor regression, although these were in the range of the GLV-1h43 treatment. For unknown reasons, the latter seemed to be more efficient than GLV-1h68 regarding tumor therapy. However, prodrug treatment could not significantly enhance the therapeutic effect, as GLV-1h43 does not encode β-galactosidase.

On the basis of the cell culture results, we have however expected stronger synergistic tumor regression effects in GLV-1h68- and prodrug-injected mice. In previous studies, two reasons, which also could apply to our tumor model system, have already been discussed regarding this discrepancy.[10] First, the authors suggested that the rapid kinetics of oncolytic VACV replication might functionally overlap with the used cytosine deaminase/5-fluorocytosine prodrug system. This might also apply to the β-galactosidase/prodrug combination that we used. Second, the authors argued that administration of 5-fluorocytosine may have inhibited the viral replication, thus reducing the antitumoral cytotoxicity induced by the oncolytic virus itself. This effect has already been reported by McCart *et al.*,[14] which is in contrast to our system, as we did not observe inhibition of viral replication in prodrug-treated animals (Supplementary Figure S3a). A reason for this difference might be extracellular activation of the β-galactosidase-activatable prodrug. The 5-fluorocytosine, on the other hand, was cleaved inside the VACV-infected cells. Therefore, the generated 5-fluorouracil may have interfered with viral replication. It would be interesting to directly compare secreted cytosine deaminase or membrane-penetrating β-galactosidase-activatable prodrugs using the currently available rVACV/GDEPT approaches to evaluate the requirements of enzyme and prodrug location in the tumor microenvironment.

Other theoretical problems could be the stability of the prodrug within the body and the immune response generated by VACV. We showed that the prodrug is not inactivated in serum containing cell culture medium; however, we cannot formally exclude a faster breakdown of the prodrug *in vivo*. The immunological effects generated by GLV-1h68 in immunocompromized nude mice as well as in an immunocompetent mouse model have been described elsewhere.[34,41–45] We do not expect immunological effects to have any influence on the described prodrug system in our model system. One could think about the generation of antibodies against β-galactosidase that could inactivate the enzyme. As we were able to show β-galactosidase activity using β-galactosidase-activated fluorescent probes in tumors of live mice (J Stritzker, M Hess *et al.*, in preparation), we think that the generation of antibodies to β-galactosidase will not have a significant role, but might

actually help to make the therapy more tumor specific, as low concentration of β-galactosidase leaking out of the tumor would be cleared efficiently.

The selectivity of certain VACV strains, such as derivates of the Lister strain, to replicate within tumor tissues lead to large tumor to background ratios of $>10^4$,[7,34] resulting in specific expression of prodrug-converting enzymes within tumor tissues. Such ratios can hardly be achieved by the use of tumor-specific antibodies, which can also be linked to prodrug-activating enzymes. Furthermore, the amount and location of functional β-galactosidase can be controlled before addition of the prodrug by fluorescent imaging using β-galactosidase-dependent probes (J Stritzker and M Hess *et al*., in preparation).

Taken together, a combined treatment using gene-directed prodrug therapy and rVACV strains such as GLV-1h68 holds great promise for successful tumor therapy; however, further research is needed to find and optimize GDEPT/rVACV systems.

## Conflict of interest

JS, NC, IG and AAS have financial interests in Genelux Corporation. CMS, UD and JBS were supported by grants of Genelux Corporation.

## Acknowledgements

The authors thank Terry Trevino, Jason Aguilar and Johanna Langbein for excellent technical assistance, Marion Adelfinger for animal care, Birgit Bergmann and Linda Böhme for antibodies, Detlev Schindler and Richard Friedel for support on flow cytometry and Andrea Feathers and Dana Haddad for editorial help. BK thanks the Deutsche Telekom Foundation for a PhD scholarship. The research was supported by Genelux Corporation, San Diego, USA.

## References

1 Lostumbo L, Carbine N, Wallace J, Ezzo J. Prophylactic mastectomy for the prevention of breast cancer. *Cochrane Database Syst Rev* 2004; CD002748.
2 American Cancer Society. Cancer facts and figures 2009. 2009. http://www.cancer.org.
3 Kumar S, Gao L, Yeagy B, Reid T. Virus combinations and chemotherapy for the treatment of human cancers. *Curr Opin Mol Ther* 2008; **10**: 371–379.
4 Vaha-Koskela MJ, Heikkila JE, Hinkkanen AE. Oncolytic viruses in cancer therapy. *Cancer Lett* 2007; **254**: 178–216.
5 Moss B. Genetically engineered poxviruses for recombinant gene expression, vaccination, and safety. *Proc Natl Acad Sci USA* 1996; **93**: 11341–11348.
6 Puhlmann M, Brown CK, Gnant M, Huang J, Libutti SK, Alexander HR *et al*. Vaccinia as a vector for tumor-directed gene therapy: biodistribution of a thymidine kinase-deleted mutant. *Cancer Gene Ther* 2000; **7**: 66–73.
7 Zhang Q, Yu YA, Wang E, Chen N, Danner RL, Munson PJ *et al*. Eradication of solid human breast tumors in nude mice with an intravenously injected light-emitting oncolytic vaccinia virus. *Cancer Res* 2007; **67**: 10038–10046.
8 Yu YA, Shabahang S, Timiryasova TM, Zhang Q, Beltz R, Gentschev I *et al*. Visualization of tumors and metastases in live animals with bacteria and vaccinia virus encoding light-emitting proteins. *Nat Biotechnol* 2004; **22**: 313–320.
9 Schepelmann S, Springer CJ. Viral vectors for gene-directed enzyme prodrug therapy. *Curr Gene Ther* 2006; **6**: 647–670.
10 Chalikonda S, Kivlen MH, O'Malley ME, Eric Dong XD, McCart JA, Gorry MC *et al*. Oncolytic virotherapy for ovarian carcinomatosis using a replication-selective vaccinia virus armed with a yeast cytosine deaminase gene. *Cancer Gene Ther* 2008; **15**: 115–125.
11 Erbs P, Findeli A, Kintz J, Cordier P, Hoffmann C, Geist M *et al*. Modified vaccinia virus Ankara as a vector for suicide gene therapy. *Cancer Gene Ther* 2008; **15**: 18–28.
12 Foloppe J, Kintz J, Futin N, Findeli A, Cordier P, Schlesinger Y *et al*. Targeted delivery of a suicide gene to human colorectal tumors by a conditionally replicating vaccinia virus. *Gene Ther* 2008; **15**: 1361–1371.
13 Gnant MF, Puhlmann M, Alexander Jr HR, Bartlett DL. Systemic administration of a recombinant vaccinia virus expressing the cytosine deaminase gene and subsequent treatment with 5-fluorocytosine leads to tumor-specific gene expression and prolongation of survival in mice. *Cancer Res* 1999; **59**: 3396–3403.
14 McCart JA, Puhlmann M, Lee J, Hu Y, Libutti SK, Alexander HR *et al*. Complex interactions between the replicating oncolytic effect and the enzyme/prodrug effect of vaccinia-mediated tumor regression. *Gene Ther* 2000; **7**: 1217–1223.
15 Puumalainen AM, Vapalahti M, Agrawal RS, Kossila M, Laukkanen J, Lehtolainen P *et al*. Beta-galactosidase gene transfer to human malignant glioma *in vivo* using replication-deficient retroviruses and adenoviruses. *Hum Gene Ther* 1998; **9**: 1769–1774.
16 Griscelli F, Opolon P, Saulnier P, Mami-Chouaib F, Gautier E, Echchakir H *et al*. Recombinant adenovirus shedding after intratumoral gene transfer in lung cancer patients. *Gene Ther* 2003; **10**: 386–395.
17 Tung CH, Zeng Q, Shah K, Kim DE, Schellingerhout D, Weissleder R. *In vivo* imaging of beta-galactosidase activity using far red fluorescent switch. *Cancer Res* 2004; **64**: 1579–1583.
18 Josserand V, Texier-Nogues I, Huber P, Favrot MC, Coll JL. Non-invasive *in vivo* optical imaging of the lacZ and luc gene expression in mice. *Gene Ther* 2007; **14**: 1587–1593.
19 Wehrman TS, von Degenfeld G, Krutzik PO, Nolan GP, Blau HM. Luminescent imaging of beta-galactosidase activity in living subjects using sequential reporter-enzyme luminescence. *Nat Methods* 2006; **3**: 295–301.
20 Lee KH, Byun SS, Choi JH, Paik JY, Choe YS, Kim BT. Targeting of lacZ reporter gene expression with radioiodine-labelled phenylethyl-beta-d-thiogalactopyranoside. *Eur J Nucl Med Mol Imaging* 2004; **31**: 433–438.
21 Louie AY, Huber MM, Ahrens ET, Rothbacher U, Moats R, Jacobs RE *et al*. *In vivo* visualization of gene expression using magnetic resonance imaging. *Nat Biotechnol* 2000; **18**: 321–325.
22 Tietze LF, Krewer B. Novel analogues of CC-1065 and the duocarmycins for the use in targeted tumour therapies. *Anticancer Agents Med Chem* 2009; **9**: 304–325.
23 Tietze LF, von Hof JM, Krewer B, Muller M, Major F, Schuster HJ *et al*. Asymmetric synthesis and biological

evaluation of glycosidic prodrugs for a selective cancer therapy. *ChemMedChem* 2008; **3**: 1946–1955.
24 Stritzker J, Weibel S, Hill PJ, Oelschlaeger TA, Goebel W, Szalay AA. Tumor-specific colonization, tissue distribution, and gene induction by probiotic *Escherichia coli* Nissle 1917 in live mice. *Int J Med Microbiol* 2007; **297**: 151–162.
25 Hirota M, Fujiwara T, Mineshita S, Sugiyama H, Teraoka H. Distamycin A enhances the cytotoxicity of duocarmycin A and suppresses duocarmycin A-induced apoptosis in human lung carcinoma cells. *Int J Biochem Cell Biol* 2007; **39**: 988–996.
26 Tada-Oikawa S, Oikawa S, Kawanishi M, Yamada M, Kawanishi S. Generation of hydrogen peroxide precedes loss of mitochondrial membrane potential during DNA alkylation-induced apoptosis. *FEBS Lett* 1999; **442**: 65–69.
27 Wrasidlo W, Johnson DS, Boger DL. Induction of endonucleolytic DNA fragmentation and apoptosis by the duocarmycins. *Bioorg Med Chem Lett* 1994; **4**: 631–636.
28 Nicholson DW, Ali A, Thornberry NA, Vaillancourt JP, Ding CK, Gallant M *et al*. Identification and inhibition of the ICE/CED-3 protease necessary for mammalian apoptosis. *Nature* 1995; **376**: 37–43.
29 Debatin KM. Apoptosis pathways in cancer and cancer therapy. *Cancer Immunol Immunother* 2004; **53**: 153–159.
30 Kim R. Recent advances in understanding the cell death pathways activated by anticancer therapy. *Cancer* 2005; **103**: 1551–1560.
31 Taylor JM, Barry M. Near death experiences: poxvirus regulation of apoptotic death. *Virology* 2006; **344**: 139–150.
32 Hurst J, Maniar N, Tombarkiewicz J, Lucas F, Roberson C, Steplewski Z *et al*. A novel model of a metastatic human breast tumour xenograft line. *Br J Cancer* 1993; **68**: 274–276.
33 Rathinavelu P, Malave A, Raney SR, Hurst J, Roberson CT, Rathinavelu A. Expression of mdm-2 oncoprotein in the primary and metastatic sites of mammary tumor (GI-101) implanted athymic nude mice. *Cancer Biochem Biophys* 1999; **17**: 133–146.
34 Gentschev I, Stritzker J, Hofmann E, Weibel S, Yu YA, Chen N *et al*. Use of an oncolytic vaccinia virus for the treatment of canine breast cancer in nude mice: preclinical development of a therapeutic agent. *Cancer Gene Ther* 2009; **16**: 320–328.
35 Boger DL, Johnson DS, Yun W, Tarby CM. Molecular basis for sequence selective DNA alkylation by (+)- and ent-(−)-CC-1065 and related agents: alkylation site models that accommodate the offset AT-rich adenine N3 alkylation selectivity. *Bioorg Med Chem* 1994; **2**: 115–135.
36 Taylor JM, Quilty D, Banadyga L, Barry M. The vaccinia virus protein F1 L interacts with Bim and inhibits activation of the pro-apoptotic protein Bax. *J Biol Chem* 2006; **281**: 39728–39739.
37 Stewart TL, Wasilenko ST, Barry M. Vaccinia virus F1L protein is a tail-anchored protein that functions at the mitochondria to inhibit apoptosis. *J Virol* 2005; **79**: 1084–1098.
38 Wasilenko ST, Banadyga L, Bond D, Barry M. The vaccinia virus F1L protein interacts with the proapoptotic protein Bak and inhibits Bak activation. *J Virol* 2005; **79**: 14031–14043.
39 Wasilenko ST, Meyers AF, Vander Helm K, Barry M. Vaccinia virus infection disarms the mitochondrion-mediated pathway of the apoptotic cascade by modulating the permeability transition pore. *J Virol* 2001; **75**: 11437–11448.
40 Wasilenko ST, Stewart TL, Meyers AF, Barry M. Vaccinia virus encodes a previously uncharacterized mitochondrial-associated inhibitor of apoptosis. *Proc Natl Acad Sci USA* 2003; **100**: 14345–14350.
41 Kelly KJ, Brader P, Woo Y, Li S, Chen N, Yu YA *et al*. Real-time intraoperative detection of melanoma lymph node metastases using recombinant vaccinia virus GLV-1h68 in an immunocompetent animal model. *Int J Cancer* 2009; **124**: 911–918.
42 Gentschev I, Hofmann E, Donat U, Weibel S, Adelfinger M, Raab V *et al*. Regression of human prostate tumors and metastases in nude mice following treatment with the recombinant oncolytic vaccinia virus GLV-1h68. *J Biomed Biotechnol* 2010; e-pub ahead of print 23 June 2010; doi:10.1155/2010/736907.
43 Worschech A, Chen N, Yu YA, Zhang Q, Pos Z, Weibel S *et al*. Systemic treatment of xenografts with vaccinia virus GLV-1h68 reveals the immunologic facet of oncolytic therapy. *BMC Genomics* 2009; **10**: 301.
44 Worschech A, Haddad D, Stroncek DF, Wang E, Marincola FM, Szalay AA. The immunologic aspects of poxvirus oncolytic therapy. *Cancer Immunol Immunother* 2009; **58**: 1355–1362.
45 Worschech A, Kmieciak M, Knutson KL, Bear HD, Szalay AA, Wang E *et al*. Signatures associated with rejection or recurrence in HER-2/neu-positive mammary tumors. *Cancer Res* 2008; **68**: 2436–2446.



Supplementary Information accompanies the paper on Cancer Gene Therapy website (http://www.nature.com/cgt)